

## Facile Synthesis, Analysis of Physico-Chemical Properties and Tape Casting of Al<sub>2</sub>O<sub>3</sub> Nanoparticles

ALAGU SEGAR DEEPI<sup>1,✉</sup>, SRINIVASAN DHARANI PRIYA<sup>1,✉</sup>,  
CLEMENTZ EDWARDRAJ FREEDA CHRISTY<sup>2,3,✉</sup> and ARPUTHARAJ SAMSON NESARAJ<sup>1,4,\*</sup>

<sup>1</sup>Department of Applied Chemistry, Karunya Institute of Technology and Sciences (Deemed to be University), Karunya Nagar, Coimbatore-641114, India

<sup>2</sup>Department of Civil Engineering, Karunya Institute of Technology and Sciences (Deemed to be University), Karunya Nagar, Coimbatore-641114, India

<sup>3</sup>Department of Civil Engineering, Kalasalingam Academy of Research and Education (Deemed to be University), Anand Nagar, Krishnankoil-626126, India

<sup>4</sup>Department of Chemistry, School of Advanced Sciences, Kalasalingam Academy of Research and Education (Deemed to be University), Anand Nagar, Krishnankoil-626126, India

\*Corresponding author: E-mail: drnesaraj@gmail.com; samson@klu.ac.in

Received: 25 May 2022;

Accepted: 30 June 2022;

Published online: 19 September 2022;

AJC-20969

Alumina (Al<sub>2</sub>O<sub>3</sub>) powder was synthesized by simple wet-chemical precipitation method. The phase study was done using XRD confirming the FCC phase. FTIR showed the presence of Al-O vibrations. Particle size analysis (PSA) confirmed the presence of particles in the range of 300 nm. The EDX confirmed the presence of Al and O elements in the samples only and no impurity elements. SEM exhibited the ultrafine nature of the particles. The tape casting of Al<sub>2</sub>O<sub>3</sub> nanoparticles was carried out with suitable organic ingredients. Based on the trials, the best composition for alumina tape casting was optimized. The SEM of green alumina thin sheet resulted in good surface behaviour. Optimized composition may be used for fabricating thin Al<sub>2</sub>O<sub>3</sub> based electrical components for application in electronics industry.

**Keywords:** Al<sub>2</sub>O<sub>3</sub>, Chemical precipitation, Physico-chemical behaviour, Tape casting, Electronics.

### INTRODUCTION

Alumina (Al<sub>2</sub>O<sub>3</sub>) ceramic is a most prominent and promising material in harsh environment (corrosion, high pressure and temperature, *etc.*) applications [1-3]. It is known for its outstanding properties such as extreme hardness, strength, corrosion resistance and reasonable cost. Numerous studies have been done based on the synthesis of ceramic alumina nanoparticles. Alumina ceramics have been used in many fields, such as, lasers, thermo-luminescence, missiles, display devices, adsorption materials, *etc.* because of their excellent material properties [4-6]. However, the above multifarious applications often require alumina ceramic with different complex shapes such as conformal, cambered, ultra-thin plates and so on.

Concerning the shaping methods, the most usual ceramic membrane fabrication methods are extrusion, pressing, sol-gel, slip casting and tape casting. Among various methods available,

tape casting is one of the reasonable and best processes employed for the manufacture of thin sheets of ceramic materials in desired thickness. It is also called as doctor blade coating [7]. Ceramic oxide particles are dispersed in solvent, forming thin ceramic sheets when coated on a uniform non-moving surface. In this technique, the particles are blended together using organic binders [8]. The main portion of procedure in tape casting is the formation of slurry, which consists of organic solvents, binders and plasticizers and dispersants. The prepared slurry is always cast on to a stationary or moving surface and dried to form a flexible ceramic sheets or tapes which can be sintered into hard ceramics for different applications. The sheets can be cut into desired shapes as per the application [9].

The 3D structures of ceramic components with flat large areas can be produced by this technique, which makes them find many industrial applications in producing materials for electronic industries, solid oxide fuel cells, batteries and

capacitors, etc. [10]. In present work,  $\text{Al}_2\text{O}_3$  nanoparticles were synthesized with a cost effective method and their physico-chemical characteristics were analyzed. The prepared  $\text{Al}_2\text{O}_3$  nanoparticles were used to prepare thin  $\text{Al}_2\text{O}_3$  flat sheet with a tape casting machine. The slurry, consisting of the alumina powder in a solvent with additives like dispersant, binder and plasticizer was cast on a stationary glass surface using a doctor blade. The green tapes were then dried with desirable mechanical characteristics. The surface phenomena of the cast alumina were analyzed.

## EXPERIMENTAL

**Synthesis of  $\text{Al}_2\text{O}_3$  nanoparticles by chemical precipitation method:** A simple chemical precipitation technique was used to synthesize  $\text{Al}_2\text{O}_3$  nanoparticles by using aluminium nitrate and sodium hydroxide as the precursor materials. The precursor materials were taken as such without any further purification. The glassware cleaned with deionized water was used throughout the experiment. Aluminium nitrate (1 M) was prepared in double distilled water with constant stirring for 1 h in a magnetic stirrer for the complete dissolution of aluminium nitrate salt. Then, freshly prepared 3 M NaOH was added in drops to the aluminium nitrate solution and stirred for about 3 h. The obtained creamy white  $\text{Al}(\text{OH})_3$  precipitate was allowed to settle down completely and washed several times with ethanol and double distilled water. The washed product was dried overnight in hot air oven maintained at 80 °C. The resultant dried product was calcined at different temperatures, such as 150, 300, 450, 600 and 800 °C for 3 h each to get purified highly crystalline  $\text{Al}_2\text{O}_3$  nanoparticles. The main reaction for the preparation of  $\text{Al}_2\text{O}_3$  nanoparticles is shown as:



**Procedure employed in tape casting technique:** Milling, casting and drying are the three processes involved in tape casting [11-14]. At the beginning, certain amount of binder and plasticizer was mixed with the solvent in a magnetic stirrer for about 2 h. After complete dissolution and mixing of the above ingredients with the solvent, alumina powder was added and milled for 3 h. Then, the dispersing agent and defoamer were added to the above slurry and again the milling was continued for another 3 h. Before casting, the viscosity of the slurry was checked in order to obtain an excellent quality green tape. The slurry with suitable consistency was poured through the cavity of the doctor's blade assembly by tape casting technique in a controlled speed [15]. The slurry was cast uniformly on a glass plate using a doctor's blade assembly in the form a thin layer with desired thickness. The tape was air dried and peeled off gently from the glass plate which resulted as a thin

flexible sheet. Further characterization was carried out using the cured ceramic tapes. The role of different ingredients involved in the tape casting of alumina nanoparticles is shown in Table-1.

**Characterization:** The XRD measurement of  $\text{Al}_2\text{O}_3$  nanoparticles was carried-out with Shimadzu XRD6000 instrument using  $\text{CuK}\alpha$  radiation with a nickel filter. The unit cell parameter was estimated by DOS software. The FTIR spectrum of  $\text{Al}_2\text{O}_3$  nanoparticles was recorded by Shimadzu (IR Prstige 21) machine. The particle size measurements for  $\text{Al}_2\text{O}_3$  nanoparticles were found by Malvern Zetasizer Ver. 6.32. The surface morphology and the elemental composition of  $\text{Al}_2\text{O}_3$  nanoparticles were studied by scanning electron microscope (SEM JEOL JSM-6610) equipped with an energy dispersive X-ray (EDX) spectrophotometer and operated at 20 kV. The tape casting of  $\text{Al}_2\text{O}_3$  nanoparticles was carried out with a desktop coating machine, Model-AC 250 (Ranga Techno Impex (P) Ltd., India). The surface morphology of the green tape was studied with the same SEM instrument.

## RESULTS AND DISCUSSION

**XRD studies:** The XRD image of the  $\text{Al}_2\text{O}_3$  nanoparticles (calcined at 800 °C for 3 h) is shown in Fig. 1. The well crystalline behavior of the  $\text{Al}_2\text{O}_3$  powder is seen in the XRD diagram. The obtained XRD data was compared with the XRD data of standard JCPDS pattern for cubic  $\text{Al}_2\text{O}_3$  (JCPDS card No. 04-0880). The XRD graph shows various diffraction peaks at  $2\theta = 37.472^\circ, 39.705^\circ, 42.859^\circ, 45.827^\circ, 60.511^\circ$  and  $67.367^\circ$  and their associated  $hkl$  values are 311, 222, 321, 400, 511, 441, respectively. The attained ' $2\theta$ ' values for the prepared  $\text{Al}_2\text{O}_3$

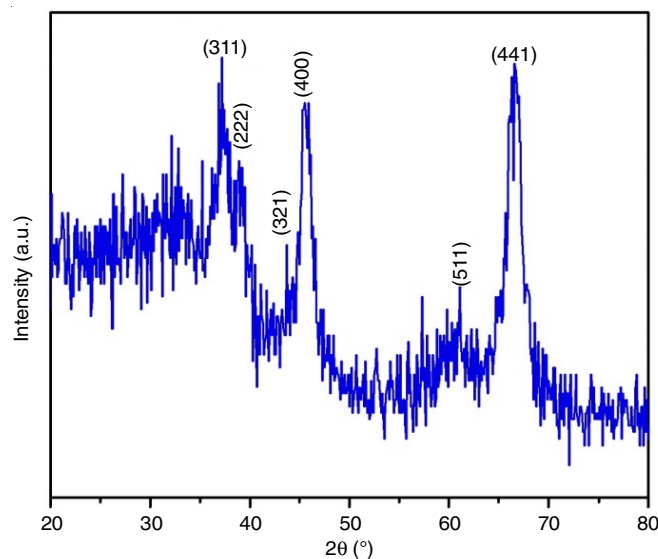


Fig. 1. XRD pattern obtained on calcined  $\text{Al}_2\text{O}_3$  nanoparticles

TABLE-1  
ROLE OF INGREDIENTS USED IN THE TAPE CASTING OF ALUMINA NANOPARTICLES

Ingredients	Function
Solvent [ethyl methyl ketone]	Dissolves organic material and act as vehicle carrying ceramic particles.
Binder [poly vinyl butyral - PVB]	Binds the ceramic particle together and strengthens the green tape.
Plasticizer [benzyl butyl phthalate - BBP]	Helps to modify viscosity, flexibility and strength of the slurry
Dispersing agent [oleic acid]	Helps in giving coating on the ceramic particles and maintains a stable suspension in the slurry.
Defoamer [silicone oil]	Improves the wetting properties of the slurry.

TABLE-2  
OBTAINED XRD DATA FOR Al<sub>2</sub>O<sub>3</sub> COMPOSITION IN COMPARISON WITH JCPDS DATA OF Al<sub>2</sub>O<sub>3</sub>

Standard XRD data for (F.C.C) Al <sub>2</sub> O <sub>3</sub> powders (JCPDS No. 04-0880)			Powder XRD data for prepared Al <sub>2</sub> O <sub>3</sub>		
2θ values	hkl values	I/I <sub>0</sub>	I/I <sub>0</sub> (obs)	hkl values	2θ values (obs)
37.472	311	40	63	311	37.320
39.705	222	20	30	222	39.500
42.859	321	30	-	321	43.737
45.827	400	20	72	400	45.825
60.511	511	10	18	511	61.100
67.367	441	100	100	441	66.923

TABLE-3  
CRYSTALLOGRAPHIC PARAMETERS OBTAINED ON Al<sub>2</sub>O<sub>3</sub> IN COMPARISON WITH STANDARD JCPDS DATA

Sample	Crystal structure	Unit cell parameter (Å)	Unit cell volume (Å <sup>3</sup> )	Crystallite size (nm)	Theoretical density (g cm <sup>-3</sup> )
Standard XRD data for (F.C.C) Al <sub>2</sub> O <sub>3</sub> (JCPDS No. 04-0880)	Cubic (F.C.)	7.95	502.46	-	3.370
Al <sub>2</sub> O <sub>3</sub>	Cubic (F.C.)	7.94	500.56	4.60	3.381

were matched well with the reported data for Al<sub>2</sub>O<sub>3</sub> and the powder was indexed to F.C.C. crystalline geometry. The achieved XRD data for Al<sub>2</sub>O<sub>3</sub> nanoparticles in comparison with JCPDS data of Al<sub>2</sub>O<sub>3</sub> is presented in Table-2.

No impurity phases were seen in the XRD data. The crystallite size (D<sub>x</sub>) was calculated by using Debye-Scherrer formula [16],

$$D_x = \frac{K\lambda}{\beta \cos \theta} \quad (2)$$

where, β is the full width at half maximum (FWHM) of a diffraction peak, K is the shape factor approx. 0.91, λ is the wavelength of the X-ray source that equals 1.54 Å and θ is the Bragg's angle. The theoretical density (D<sub>p</sub>) was calculated by using the formula:

$$D_p \text{ (g cm}^{-3}\text{)} = \frac{Z \times M}{N \times V} \quad (3)$$

where, Z is the number of chemical species in the unit cell, M is the molecular mass of the sample (g/mol), N is the Avogadro's number (6.023 × 10<sup>23</sup>) and V is the unit cell volume equals to a<sup>3</sup> which is the lattice constant in cm. The crystallographic parameters obtained on Al<sub>2</sub>O<sub>3</sub> nanoparticles are shown in Table-3.

**FTIR studies:** Fig. 2 shows the FTIR spectrum obtained on Al<sub>2</sub>O<sub>3</sub> nanoparticles prepared by the chemical precipitation method. The band appeared at 3466.18 cm<sup>-1</sup> is ascribed to O-H stretching due to water. The band appeared at 1646.71 region is due to O-H bending vibrations. The weak peaks appeared at 1380.24, 854.21 and 595.52 cm<sup>-1</sup> are corresponded to Al-O (M-O) bond vibrations [17]. Band assignment in Al<sub>2</sub>O<sub>3</sub> nanoparticles by FTIR spectrum is shown in Table-4.

**Particle size analysis (PSA):** The prepared Al<sub>2</sub>O<sub>3</sub> nanoparticles (after calcination at 800 °C for 3 h) subjected to particle size measurements using triple distilled water as medium. For the measurement, the sample was sonicated in triple distilled water for about 10 min and after that the sample was subjected for particle size analysis. The particle size distribution curve obtained on Al<sub>2</sub>O<sub>3</sub> nanoparticles is shown in Fig. 3. The particle size distribution of Al<sub>2</sub>O<sub>3</sub> is in the range of 300 nm indicating

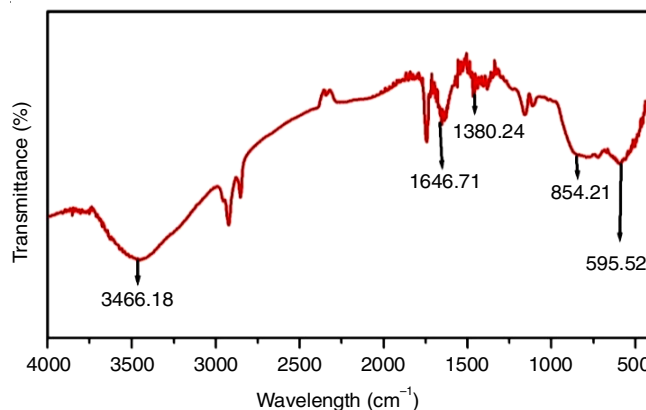


Fig. 2. FTIR spectrum obtained on Al<sub>2</sub>O<sub>3</sub> based nanoparticles

TABLE-4  
BAND ASSIGNMENT IN Al<sub>2</sub>O<sub>3</sub> NANOPARTICLES BY FTIR SPECTRUM

Wavenumber (cm <sup>-1</sup> )	Band assignment
3466.18	O-H stretching
1646.71	O-H bending vibration
1380.24	M-O bonding
854.21	M-O bonding
595.52	M-O bonding

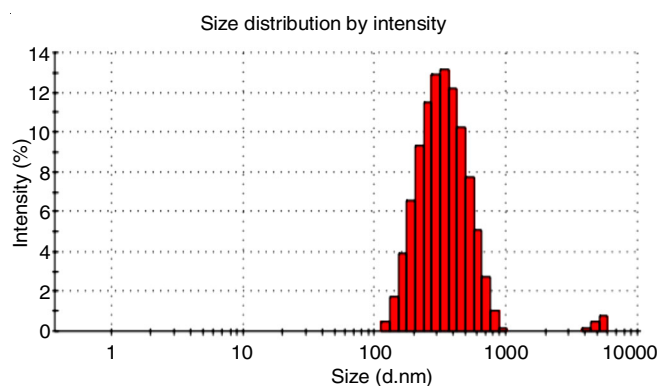


Fig. 3. Particle size analysis pattern obtained on Al<sub>2</sub>O<sub>3</sub> nanoparticles

uniform heat treatment. The particle size data obtained on Al<sub>2</sub>O<sub>3</sub> nanoparticles is presented in Table-5.

TABLE-5 PARTICLE SIZE DATA OBTAINED ON $\text{Al}_2\text{O}_3$ NAOPARTICLES						
Peak 1			Peak 2			Average particle size (nm)
Intensity (%)	Diameter (nm)	Width (d.nm)	Intensity (%)	Diameter (nm)	Width (d.nm)	
98.6	356.5	146.1	1.4	5174	488.4	310.9

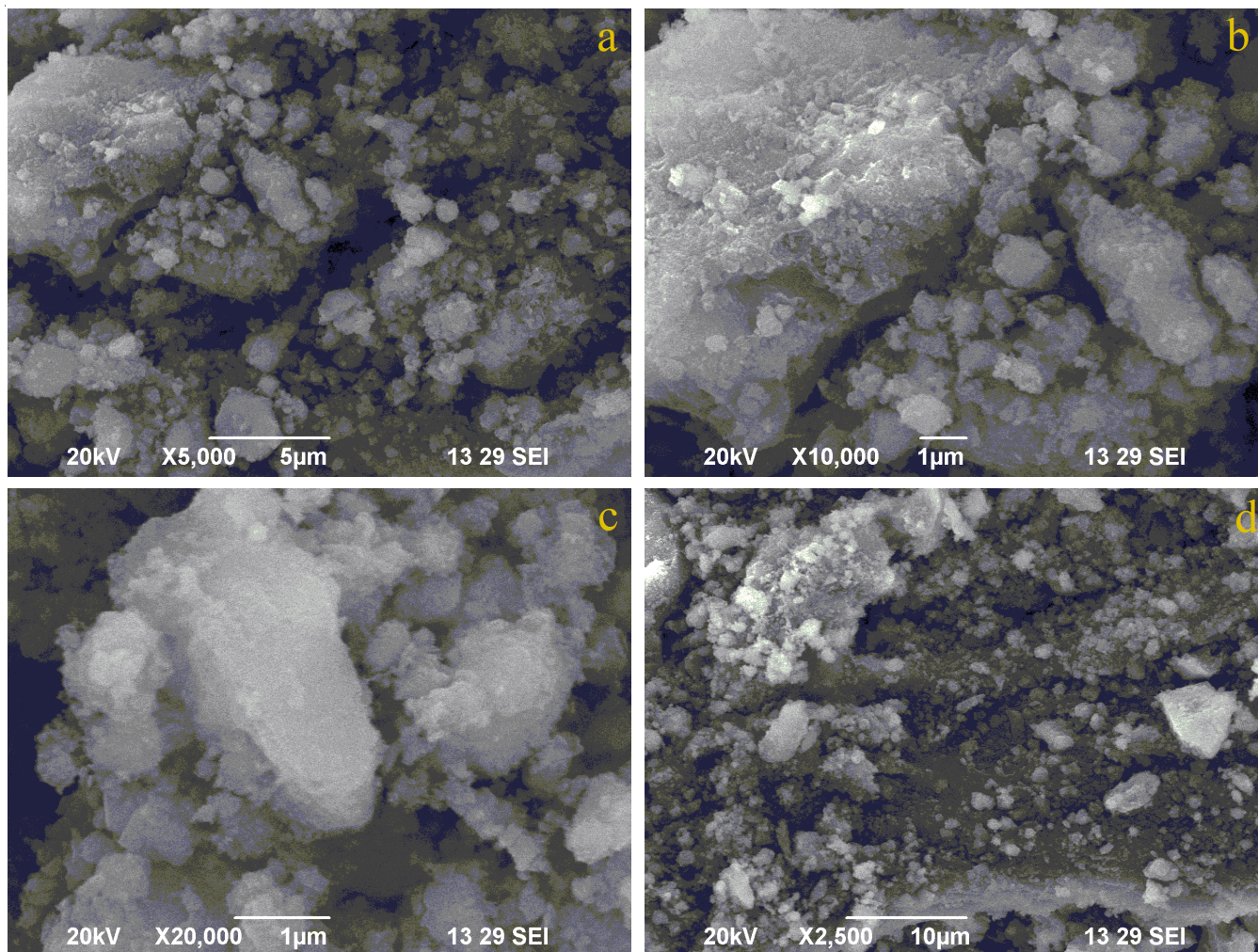


Fig. 4. SEM photographs obtained on  $\text{Al}_2\text{O}_3$  nanoparticles

**Scanning electron microscopy (SEM) studies:** The SEM images obtained on  $\text{Al}_2\text{O}_3$  nanoparticles are shown in the Fig. 4(a-d). It is found that the grains are not uniform having irregular shapes. Also, the agglomeration effect can be seen in all the SEM pictures.

**Energy dispersive X-ray analysis (EDX) studies:** The elemental composition of synthesized  $\text{Al}_2\text{O}_3$  nanoparticles was observed using EDX spectroscopy. The purity of aluminium oxide is reflected in the quantitative measurements derived from EDX analysis. The EDX measurements revealed the existence of Al and O peaks with no additional peaks indicating the formation of  $\text{Al}_2\text{O}_3$  [18] (Fig. 5). The elemental composition data obtained on  $\text{Al}_2\text{O}_3$  nanoparticles is given in Table-6.

**Fabrication of  $\text{Al}_2\text{O}_3$  thin films by tape casting technique:** To optimize the exact composition of ingredients in preparing the slurry, the trials were employed. The composition of the trials and the resultant quality of green tapes are presented in

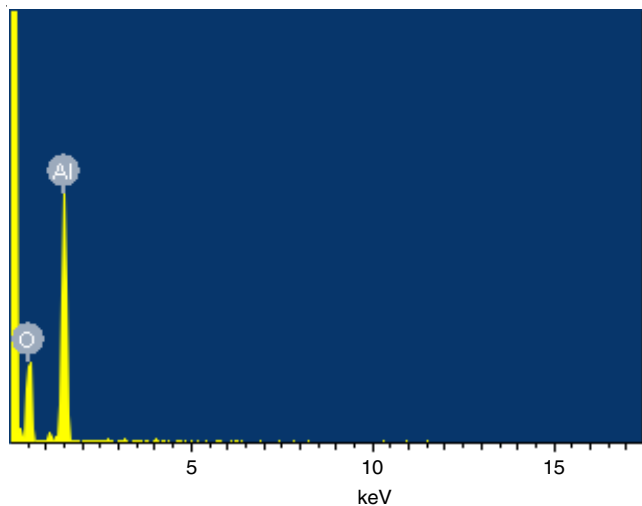


Fig. 5. EDX spectrum obtained on  $\text{Al}_2\text{O}_3$  nanoparticles

TABLE-6  
ELEMENTAL COMPOSITION DATA  
OBTAINED ON  $\text{Al}_2\text{O}_3$  NANOPARTICLES

Element	Weight (%)	Atomic (%)
O	53.93	66.38
Al	46.07	33.62

Table-7. In the initial trial (AO-I), the green tape resulted with pinholes after drying because of less amount binder and less volume of solvent. However, the green tape was easily removed from the glass plate after complete removal of solvent from it. The quality of the  $\text{Al}_2\text{O}_3$  tape based on trial AO-I was not good.

In the next trial (AO-II), the quantity of the ceramic powder was slightly increased along-with the slight raise in the binder content and an enhanced volume of the solvent. It was reported that the amount of binder in the green tapes clearly influences

the packing of ceramic particles [19]. The milling was carried out in the same manner with a magnetic stirrer and the casting was carried-out in the glass plate. After drying, the  $\text{Al}_2\text{O}_3$  tape based on AO-II was resulted with good quality without any pinholes. The tape was highly flexible also. The best quality of  $\text{Al}_2\text{O}_3$  thin film may be due to the presence of optimized ingredients in the slurry. The surface microstructure of the green  $\text{Al}_2\text{O}_3$  thin film produced by AO-II composition is shown in Fig. 6. SEM photographs depict the typical microstructure of the green  $\text{Al}_2\text{O}_3$  tape having smooth defect-free surface, which is believed to be attributed to the well dispersed and stable slurry. The homogenous particle packing of the green tape was shown by SEM (Fig. 6). From this study, it was found that this optimized composition may be utilized to fabricate thin film of any ceramic material for application in electronics, sensors, energy devices, dielectric components, *etc.*

TABLE-7  
EXPERIMENTAL COMPOSITION USED FOR THE TAPE CASTING OF  $\text{Al}_2\text{O}_3$  CERAMICS

Tape code	Ceramic powder (g)	PVB (g)	BBP (mL)	Oleic acid (mL)	Silicone oil (drops)	Ethyl methyl ketone (mL)	Green tape quality
AO-I	5	2.5	1.8	0.50	3	15	Pinholes resulted
AO-II	6	5	1.8	0.50	3	30	Good

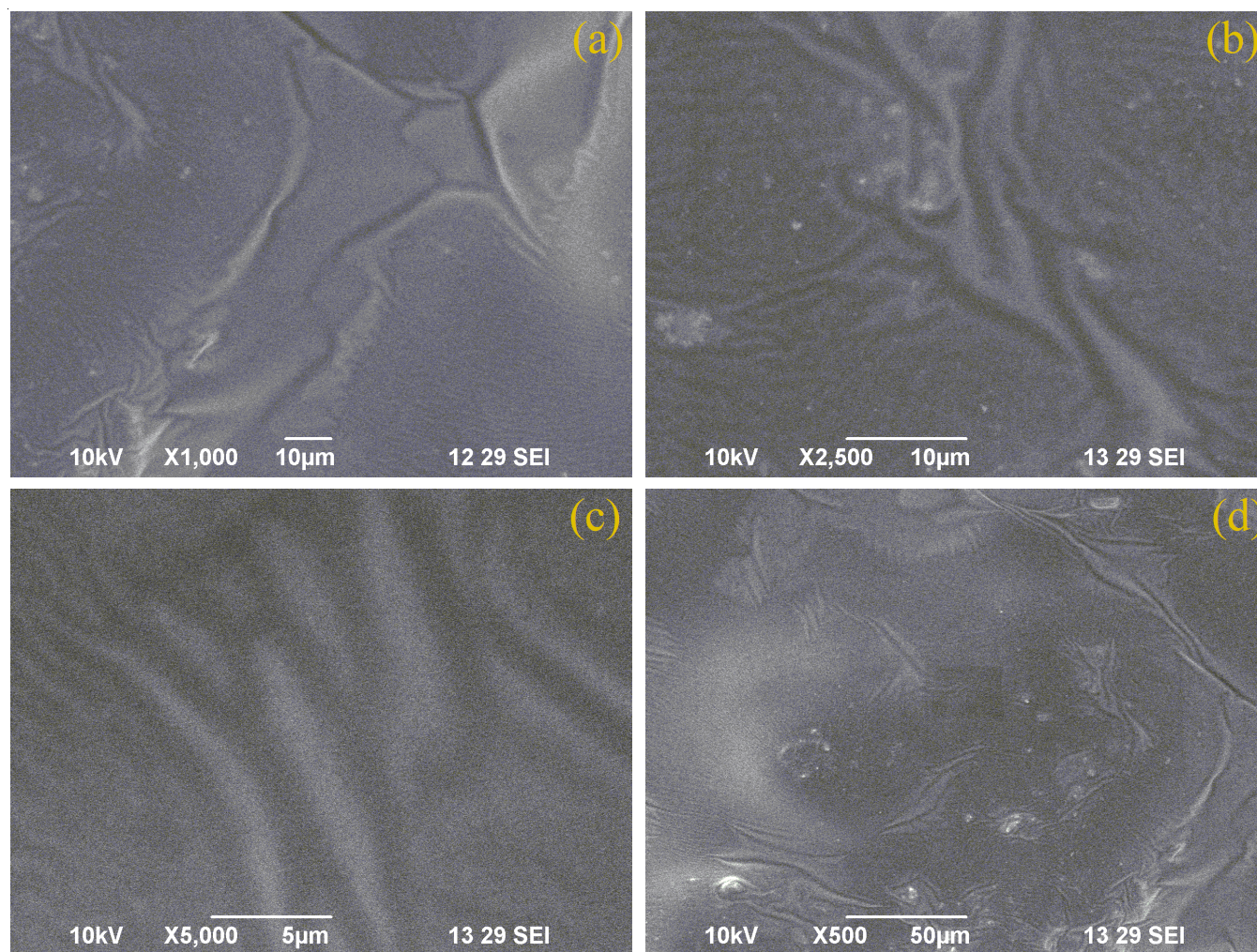


Fig. 6. SEM images of  $\text{Al}_2\text{O}_3$  thin film prepared by tape casting (AO-II)

## Conclusion

To sum up this work, Al<sub>2</sub>O<sub>3</sub> nanoparticles were synthesized by a simple chemical precipitation method with cheap chemicals. The structural, functional, particulate, microstructural and elemental characteristics were studied by XRD, FTIR, particle size analysis, SEM and EDX techniques. The XRD of the sample resulted in FCC structure. The Al-O bonding was confirmed by FTIR analysis. The particle diameter of the sample was found to be 300 nm and the non-uniform grains were detected from SEM analysis. Presence of Al and O was confirmed by EDX. Al<sub>2</sub>O<sub>3</sub> thin film was fabricated by tape casting technique with appropriate binder, plasticizer, dispersing agent and defoamer. The optimized composition of Al<sub>2</sub>O<sub>3</sub> thin film may be used for fabrication of any ceramic thin film for electronics, dielectrics and other advanced applications.

## ACKNOWLEDGEMENTS

The authors thank Central Power Research Institute (Ministry of Power, Govt. of India) (Grant No.CPRI/R&D/TC/GDEC/2019, dated 06-02-2019) for the financial support. One of the authors, ASN acknowledges the Management of Karunya Institute of Technology and Sciences for providing the necessary facilities to initiate Fuel Cell research activity in the Department of Applied Chemistry.

## CONFLICT OF INTEREST

The authors declare that there is no conflict of interests regarding the publication of this article.

## REFERENCES

1. Y. Yang and Y. Wu, *J. Mater. Res.*, **29**, 2312 (2014); <https://doi.org/10.1557/jmr.2014.225>
2. Y. Sun, S. Shimai, X. Peng, M. Dong, H. Kamiya and S. Wang, *J. Mater. Res.*, **29**, 247 (2014); <https://doi.org/10.1557/jmr.2013.381>
3. Z. Feng, J. Qi, Y. Han and T. Lu, *Ceram. Int.*, **44**, 1059 (2018); <https://doi.org/10.1016/j.ceramint.2017.10.048>
4. N.A. Ghulam, M.N. Abbas and D.E. Sachit, *Indian Chem. Eng.*, **62**, 301 (2020); <https://doi.org/10.1080/00194506.2019.1677512>
5. M.G. Ghoniem, T.M. Sami, S.A. El-Reefy and S.A. Mohamed, *WIT Transac. Ecol. Environ.*, **180**, 29 (2014); <https://doi.org/10.2495/WM140031>
6. L. Liu, S. Luo, B. Wang and Z. Guo, *Appl. Surf. Sci.*, **345**, 116 (2015); <https://doi.org/10.1016/j.apsusc.2015.03.145>
7. R.K. Nishihora, P.L. Rachadel, M.G.N. Quadri and D. Hotza, *J. Eur. Ceram. Soc.*, **38**, 988 (2018); <https://doi.org/10.1016/j.jeurceramsoc.2017.11.047>
8. M. Boussemghoune, M. Chikhi, Y. Ozay, P. Guler, B. Ozbey-Unal and N. Dizge, *Symmetry*, **12**, 770 (2020); <https://doi.org/10.3390/sym12050770>
9. P. Wicinska, T. Graule and M. Bachonko, *J. Eur. Ceram. Soc.*, **35**, 3949 (2015); <https://doi.org/10.1016/j.jeurceramsoc.2015.05.028>
10. Z. Feng, J. Qi and T. Lu, *J. Eur. Ceram. Soc.*, **40**, 1168 (2020); <https://doi.org/10.1016/j.jeurceramsoc.2019.11.065>
11. A.S. Nesaraj, I.A. Raj and R. Pattabiraman, *Indian J. Eng. Mater. Sci.*, **9**, 58 (2002).
12. J.-H. Jean and H.-R. Wang, *J. Am. Ceram. Soc.*, **81**, 1589 (1998); <https://doi.org/10.1111/j.1151-2916.1998.tb02521.x>
13. N. Suppakarn, H. Ishida and J.D. Cawley, *J. Am. Ceram. Soc.*, **84**, 289 (2001); <https://doi.org/10.1111/j.1151-2916.2001.tb00652.x>
14. Y.-P. Zeng, D.-L. Jiang and T. Watanabe, *J. Am. Ceram. Soc.*, **83**, 2999 (2000); <https://doi.org/10.1111/j.1151-2916.2000.tb01673.x>
15. M. Boaro, J.M. Vohs and R.J. Gorte, *J. Am. Ceram. Soc.*, **86**, 395 (2003); <https://doi.org/10.1111/j.1151-2916.2003.tb03311.x>
16. R. Vijayalakshmi and V. Rajendran, *Arch. Appl. Sci. Res.*, **4**, 1183 (2012).
17. N. Varghese, M. Hariharan, A.B. Cherian, P.V. Sreenivasan, J. Paul and K.A. Asmy Antony, *Int. J. Sci. Res.*, **4**, 1 (2014).
18. D. Manyasree, P. Kiranmayi and R.V.S.S.N. Ravikumar, *Int. J. Pharm. Pharm. Sci.*, **10**, 32 (2018); <https://doi.org/10.22159/ijpps.2018v10i1.20636>
19. M. Rauscher and A. Roosen, *J. Am. Ceram. Soc.*, **6**, 24 (2009); <https://doi.org/10.1111/j.1744-7402.2008.02314.x>